AAPT PHYSICS EDUCATION | AMERICAN JOURNAL of PHYSICS

Wave physics of the graphene lattice emulated in a ripple tank

J. Rössler, C. Rössler, P. Märki, K. Ensslin, and T. Ihn

Citation: American Journal of Physics **83**, 761 (2015); doi: 10.1119/1.4923445
View online: http://dx.doi.org/10.1119/1.4923445
View Table of Contents: http://scitation.aip.org/content/aapt/journal/ajp/83/9?ver=pdfcov
Published by the American Association of Physics Teachers

Wave physics of the graphene lattice emulated in a ripple tank

J. Rössler, C. Rössler, P. Märki, K. Ensslin, and T. Ihn
Solid State Physics Laboratory, ETH Zürich, 8093 Zürich, Switzerland

(Received 19 March 2015; accepted 23 June 2015)

Using the example of graphene, we have extended the classic ripple tank experiment to illustrate the behavior of waves in periodic lattices. A loudspeaker driving air through a periodically perforated plate onto the tank's water surface creates wave patterns that are in agreement with numerical simulations and are explained in terms of solid state theory. From an educational point of view, the experiment provides an illustrative example of the concepts of reciprocal space and symmetry. © *2015 American Association of Physics Teachers.*
[http://dx.doi.org/10.1119/1.4923445]

I. INTRODUCTION

At public outreach events as well as in schools and undergraduate lectures, the ripple tank is widely used to illustrate wave phenomena.[1,2] However, a standard ripple tank's hardware accessories cannot create patterns that illustrate the behavior of waves in periodic lattices. This challenged us to modify the setup in a way that provides multiple periodic sources. Employing a loudspeaker and a PMMA plate with hexagonally arranged holes, we were able to realize wave patterns in the ripple tank that are reminiscent of the microscopic images of artificial graphene.[3] Two characteristic interference patterns are depicted in Fig. 1. Readers familiar with solid state physics will recognize the same symmetry as graphene electronic wave functions in the center of the first Brillouin zone. We find that the strongest interference patterns are not obtained when the excitation wavelength is equal to the nearest-neighbor separation a_0. Instead, the symmetry of the lattice favors wavelengths that are 13.4% shorter than a_0. This discrepancy hints at the nontrivial symmetry properties of the honeycomb lattice and is explained by means of solid state theory, testifying to the applicability of our ripple tank for educational purposes.

The paper is organized as follows: Sec. II describes the technical details of the setup; in Secs. III and IV we describe single and double-hole experiments; and in Sec. V, the favorable excitation wavelengths are extracted from the discrete Fourier transform of a finite honeycomb lattice. Section VI targets the correspondence between water waves in the ripple tank and electronic wave functions in graphene. We close with a summary and outlook.

II. SETUP

Figure 2 shows the modified ripple tank setup. A loudspeaker is used as a precise and inexpensive source of excitation;[4] it is mounted face-down inside a PMMA hood. An aluminum rack holds both the hood and an interchangeable source plate $295 \times 295 \times 4.2$ mm^3 in size. The source plate shown in Fig. 2 is patterned with a honeycomb lattice of holes. Directly underneath the source plate, we place a commercially available ripple tank (Leybold, No. 401 501, with see-through water trough, tilted mirror, and observation screen). The distance between source plate and water surface is only a few millimeters. A white LED mounted in front of the center of the loudspeaker illuminates the ripple tank surface and can be used as a stroboscope to observe the wave pattern at fixed phase. To that end, the LED is typically powered for 1% of each wave cycle, thus allowing the observation of the wave during a 4° phase interval.

The stroboscope's and the loudspeaker's frequencies, their relative phase-shift, the wave form, and the amplitude are controlled using a LabView program on a standard PC via a USB Audio Adapter (LogiLink, UA0078). Between PC and loudspeaker or stroboscope, amplifiers are used to scale the signals appropriately. The loudspeaker requires between 0.3 V and 3 V ac input voltage, the LED 4 V dc. The loudspeaker receives a sinusoidal input signal; the stroboscope's waveform is set to rectangular.

In combination with the loudspeaker, the hole pattern of the source plate thus creates a controlled spatial pattern of point sources of sinusoidal-in-time air blasts directed

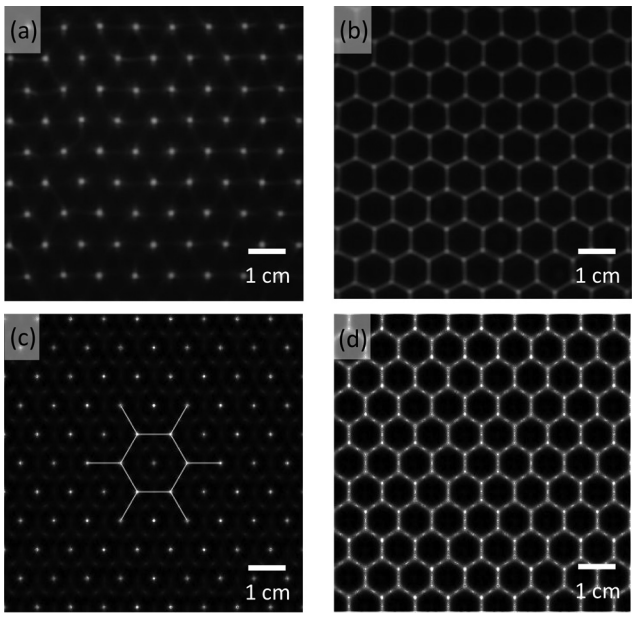

Fig. 1. (a) Photograph of the observation screen picturing the ripple tank's surface while driving air through a PMMA plate with 660 hexagonally arranged holes; the next-neighbor distance is $a_0 = 1$ cm. The excitation frequency that generates the sharpest patterns corresponds to a wavelength in water of $\lambda = \sqrt{3}/2$ cm. (b) As in (a), but with an additional phase difference of π between excitation and the stroboscope. The centers of the dark hexagons correspond to the bright spots in (*a*). Over time, the wave oscillates back and forth between these patterns. (c) and (d) show simulation results of the 2D wave pattern obtained by solving the wave equation for 660 time-harmonic sources in a water-like environment [see Eq. (2)]; parameters are the same as in (a) and (b), respectively. The white lines in (c) indicate the honeycomb pattern of the source plate.

downward onto the surface of the water.[5] Since ripple crests/valleys act on the illuminating light as converging/diverging lenses,[6] the resulting wave pattern on the water surface becomes visible as bright and dark areas projected onto the observation screen.

III. SINGLE SOURCE

We performed a series of single-source experiments to determine the dispersion relation of water waves in our setup. The water height in the tank was kept constant at $h = 1.8\,\text{cm}$, and the wavelength was between 0.5 cm and 2.5 cm. Since wavelength and water height are of the same order of magnitude, the dispersion relation for ripples is to a good approximation[7] given by

$$\omega^2 = gk + \frac{Sk^3}{\rho}, \tag{1}$$

where ω is the angular frequency of the ripple, $k = 2\pi/\lambda$ is the wavevector, ρ is the density of the water ($1\,\text{g/cm}^3$), S is the surface tension ($73\,\text{g/s}^2$), and g is the absolute value of the gravitational field strength ($981\,\text{cm/s}^2$).

For single-source experiments, we fabricated a source plate with a single hole 2 mm in diameter. The frequency was swept from 5 to 40 Hz and the observation screen was photographed using a digital camera; Fig. 3(a) shows an example photo. The radial distance between two adjacent bright circles in Fig. 3(a) is the wavelength. Figure 3(b) shows our measured wavelengths in comparison to a plot of Eq. (1). For frequencies above 10 Hz, we find a good agreement; the deviation at low excitation frequencies could be caused by operating the loudspeaker outside its specified range, which might introduce nonlinearities in the excitation. Fitting the data using least mean squares, we extract a measurement uncertainty of $\sigma = 1\,\text{Hz}$ for each data point, assuming that all uncertainties are statistical in nature. Measurement uncertainties comprise calibration errors of the gauge scale on the observation screen, reading errors of the wavelength, and calibration errors of the frequency generator. Thus, for example, at 30 Hz, the wavelength generated by our setup is known with 0.02 cm precision.

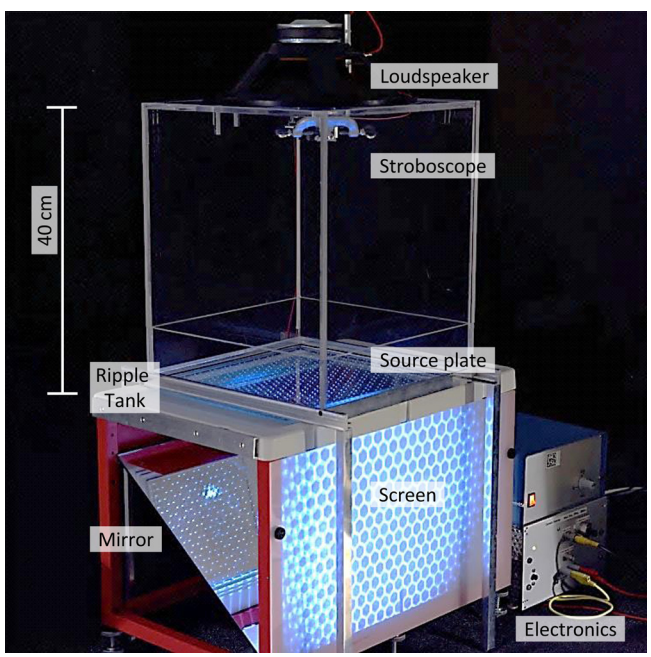

Fig. 2. Setup of the ripple tank showing a 2D honeycomb wave pattern. Sound waves travel from the loudspeaker (top) through the hexagonally patterned source plate onto the ripple tank's surface. The image is created by using a stroboscopic LED (top) that projects the wave pattern via the mirror onto the screen.

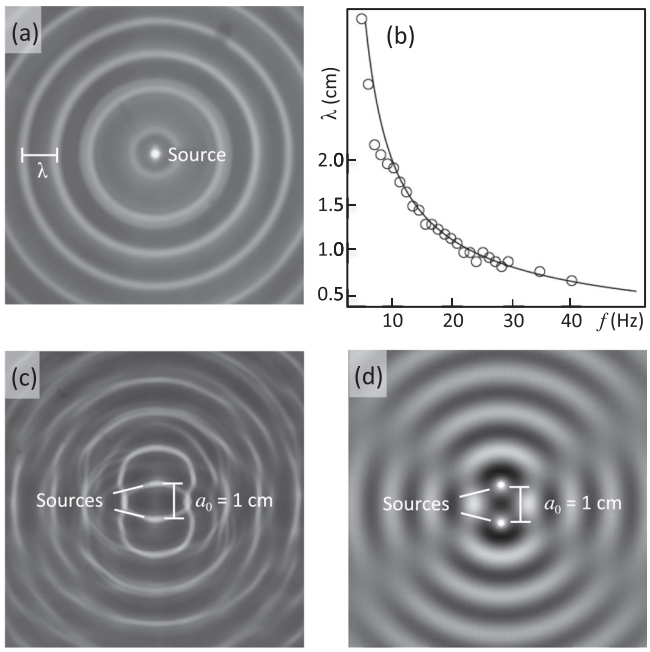

Fig. 3. (a) Photograph of the observation screen for a single-point-source plate at $\lambda = 1$ cm. (b) Measured (circles) and calculated [curve, from Eq. (1)] dispersion relation in the ripple tank. (c) Photograph of the observation screen for a double-point-source plate at $\lambda = 1$ cm. (d) Simulation of the 2D wave pattern created by two time-harmonic sources in a water-like environment.

IV. TWO SOURCES

Using a plate with two holes, we can emulate a double-slit experiment. We choose this well-known geometry to compare measurement with simulation as well as to study the effect the nonzero hole diameter has on the pattern.

The angles of constructive and destructive interference[8] can be read from Fig. 3(c). Starting with the solution to the wave equation of a 2D time-harmonic source[12] for a radially propagating wave,

$$\psi(r,k,\omega,t) = \frac{-i}{2\pi\sqrt{2}}\left[H_0^2(kr)e^{i\omega t} + H_0^2(-kr)e^{-i\omega t}\right], \tag{2}$$

with H_0^2 the zero-order Hankel function of the second kind, k the absolute value of the wave vector, r the radial distance from the source, ω the radial frequency, and t the time, we performed a Mathematica-based simulation of the 2D wave pattern. The result of these calculations is shown in Fig. 3(d).

To estimate the effect of the nonzero hole size, we compare a simulated wave function $\psi_1(x,y)$ with two point-like sources to a wave function $\psi_2(x,y)$ where each source is replaced by five sources at the four endpoints and the center of a crosshair whose diameter corresponds to the diameter of the holes. As a figure of merit, we introduce the correlation between $\psi_1(x,y)$ and $\psi_2(x,y)$

$$\zeta = \frac{\langle \psi_1(x,y)\, \psi_2(x,y) \rangle}{\sqrt{\langle |\psi_1(x,y)|^2 \rangle \langle |\psi_2(x,y)|^2 \rangle}}. \tag{3}$$

Using a distance between the sources of $a_0 = 1$ cm and a hole diameter of 2 mm, we find ζ to be 99.7%. Since these parameters are also convenient to realize experimentally, we use them with confidence in all subsequent source plates.

V. HONEYCOMB LATTICE

The symmetry properties of the honeycomb lattice can be inferred by performing the Fourier transform of the wave pattern. We use the fact that this transform can be expressed as the product of the Fourier transform of a single time-harmonic point source and that of the lattice. We perform a discrete Fourier transform of a finite lattice and compare the results to key parameters known from the Fourier transform of an infinite lattice, which are deduced from the pseudopotential method for a crystal with a two-atom basis.[11]

We created a 42-point lattice with $a_0 = 1$ cm for the discrete transform; Fig. 4(a) shows this lattice in real space while Fig. 4(b) shows the squared modulus of its discrete Fourier transform. As expected from the pseudopotential method we find a pattern with two classes of points with an intensity ratio of 1 to 4. The short (purple) arrows indicate the six shortest reciprocal lattice vectors $\vec{b}_1$, $\vec{b}_2$, $-\vec{b}_1$, $-\vec{b}_2$, $\vec{b}_1 - \vec{b}_2$, and $-\vec{b}_1 + \vec{b}_2$, with

$$\vec{b}_1 = \frac{2\pi}{a_0\sqrt{3}} \begin{pmatrix} 1 \\ 1/\sqrt{3} \end{pmatrix}, \quad \vec{b}_2 = \frac{2\pi}{a_0\sqrt{3}} \begin{pmatrix} 0 \\ 2/\sqrt{3} \end{pmatrix}, \tag{4}$$

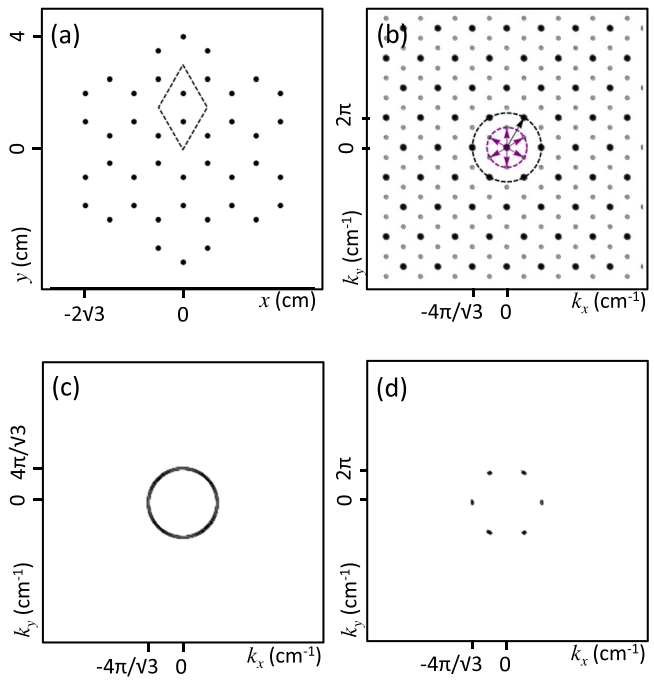

Fig. 4. (a) Honeycomb pattern with 42 holes; the nearest-neighbor distance a_0 is 1 cm; dashed black lines indicate the unit cell of the lattice. (b) 2D discrete Fourier transform of the pattern depicted in (a); dark spots correspond to high amplitude. The short arrows indicate the six lowest reciprocal lattice vectors, while the long arrow indicates the next-highest reciprocal lattice vector. (c) 2D discrete Fourier transform of a single time-harmonic source with wavelength $\lambda = \sqrt{3}/2$ cm. (d) 2D discrete Fourier transform of 42 time-harmonic point sources with wavelengths $\lambda = \sqrt{3}/2$ cm.

and correspond to the weak intensity points in the pattern. The long (black) arrow indicates the next longer reciprocal lattice vector $\vec{b}_1 + \vec{b}_2$. The radii of the dashed circles in pink and black correspond to the k-vector lengths favored by the pattern, while all other lengths are suppressed. The finite lattice size employed in the calculation manifests itself in the width of the points.

The discrete 2D Fourier transform of a single time-harmonic point source is shown in Fig. 4(c) for the specific wavelength of $\sqrt{3}/2$ cm. We see a circle of radius $4\pi/\sqrt{3}$ cm^{-1}. The final result, the 2D Fourier transform of the 42 time-harmonic point sources, is shown in Fig. 4(d), which depicts the product of the Fourier transforms shown in Fig. 4(b) and Fig. 4(c). Consequently, the discrete 2D Fourier transform of Fig. 1(a), which was taken at an excitation wavelength of $\lambda = \sqrt{3}/2$ cm, yields six points on a circle in k-space, analogous to Fig. 4(d).

This analysis illustrates that the resulting wave pattern in real space is, at the given wavelength, essentially a superposition of six plane-wave states. In general, the excitation wavelength, which determines the radius of the circle in Fig. 4(c), therefore, serves as a tool to select the finite set of plane-wave states that superimpose in real space. Most importantly, it is not the correspondence between the nearest-neighbor separation and the wavelength in real space that gives rise to strong interference patterns, as one could naively think. Instead, the wavelength of strongest interference, $\lambda = (\sqrt{3}/2)\, a_0$, corresponds to half the side length of the rhombus drawn as a dashed line in Fig. 4(a). Thus, the lattice ripple tank experiment leads to the conclusion that the rhombus and not the honeycomb is the unit cell of the graphene lattice.[9] The rhombus is the smaller and thus more fundamental unit from which any honeycomb lattice can be constructed.

VI. CORRESPONDENCE TO GRAPHENE

In the present experimental setting, all sources are in phase, since they are excited by a common air pulse. This means that as far as the correspondence to graphene is concerned, we are limited to mimicking wave functions consisting of counterpropagating waves at the Γ-point.

The strongest resonance in the ripple tank is excited with $\lambda = (\sqrt{3}/2)a_0$. As discussed in Sec. V, this corresponds to k-vectors of length $k = 4\pi/(\sqrt{3}a_0)$. There is a superposition of six basis vectors of the reciprocal lattice with this k-vector length [see Fig. 4(b)]. Labeling them consecutively by $\vec{\Lambda}_1$

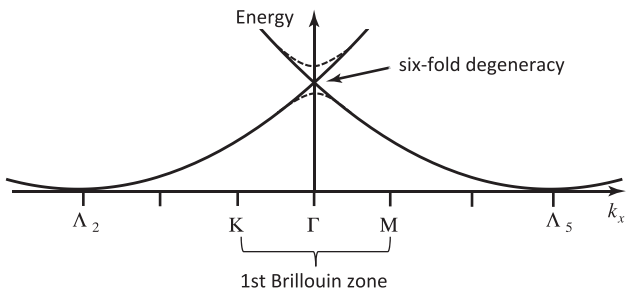

Fig. 5. Cut through the 2D band structure of graphene along the k_x-direction (schematic drawing). On the horizontal axis, the symmetry points and the first Brillouin zone are indicated. The dashed curves indicate the lifting of the degeneracy due to the atomic potential.

through $\vec{\Lambda}_6$ in the clockwise direction and solving the Schrödinger equation for graphene in the empty lattice approximation, we can draw the 2D band structure that consists of six parabolic dispersion relations all crossing at the Γ-point.[11] Figure 5 shows a cut along the $\vec{\Lambda}_2$–$\vec{\Lambda}_5$ direction, which coincides with the k_x-direction. Beyond the empty lattice approximation, the six-fold degeneracy at the Γ-point is lifted by taking the atomic potential into account. The lowest-lying band, which is the symmetric combination of all six basis states with wave-vectors Λ_1 to Λ_6, and therefore the only combination without phase differences between the waves, corresponds to the symmetry of the water waves and will therefore exhibit the same symmetry as the honeycomb pattern shown in Fig. 1.

VII. SUMMARY AND OUTLOOK

With a modification that provides periodic sources, we have extended the classic ripple-tank experiment to illustrate symmetry properties of the honeycomb lattice. The experimentally observed patterns can be reproduced closely by numerical simulations. A next step could be to introduce phase shifts between the individual point sources. However, this would require a completely new excitation technique. A more promising application for the present technique is to mimic electron waves in cavities.[10] In this case, the apparatus could not only be used to make current science accessible to students or the general public but might also prove to be a useful modeling tool for microstructured geometries that are costly and time-consuming to fabricate.

ACKNOWLEDGMENTS

The authors thank D. Bischoff and I. Blatter for fruitful discussions. This work was supported by NCCR Quantum Science and Technology (NCCR QSIT), a research instrument of the Swiss National Science Foundation (SNSF).

[1]G. Kuwabara, T. Hasegawa, and K. Kono, "Water waves in a ripple tank," Am. J. Phys. **54**, 1002–1007 (1986).
[2]F. Logiurato, "New experiments on wave physics with a simply modified ripple tank," Phys. Teach. **52**, 228–231 (2014).
[3]K. K. Gomes, W. Mar, W. Ko, F. Guinea, and H. C. Manoharan, "Designer Dirac fermions and topological phases in molecular graphene," Nature **483**, 306–310 (2012).
[4]R. Greene, "Loudspeakers as ripple tank wave generators," Am. J. Phys. **45**, 683–684 (1977).
[5]W. Baldwin, "A stroboscopic ripple tank," Rev. Sci. Instrum. **1**, 309–324 (1930).
[6]T. B. Greenslade, "Surface bubbles in the bathtub and reflections on ripple tanks," Phys. Teach. **50**, 17 (2012).
[7]C. B. Clark, "Speed of straight waves in a ripple tank," Am. J. Phys. **27**, 478–483 (1959).
[8]D. H. C. Poon, "How good is the approximation," Phys. Teach. **40**, 460–462 (2002).
[9]P. R. Wallace, "The band theory of graphite," Phys. Rev. **71**, 622–634 (1947).
[10]C. Rössler *et al.*, "Spin-coherent dot-cavity electronics," e-print arXiv:1503.02928 (2015).
[11]T. Ihn, *Semiconductor Nanostructures* (Oxford U.P., Oxford, 2010), Chap. 3.1, pp. 22–23.
[12]K. Watanabe, *Integral Transform Techniques for Green's Function* (Springer, New York, 2014), Chap. 2, pp. 28–34.

Arc Lamp Unit

At the beginning of the twentieth century, the light source for a magic lantern (slide projector) could be an oxy-hydrogen flame directed on a block of limestone (the lime-light), or a high-wattage electric lamp or an arc lamp. In many cases the large, sheet-metal casing of the lantern could accommodate any one of these three sources. Notice the complex series of bevel gears used to adjust the carbons to give the necessary gap in which the plasma arc is formed. Jack Judson of San Antonio, an expert collector of magic lanterns and slides, tells me that this example, by A. T. Thompson of Boston, was made in 1900, plus or minus ten years. (Notes and photograph by Thomas B. Greenslade, Jr., Kenyon College.)